Arch. Mech., 43, 5, pp. 623–651, Warszawa 1991

Axisymmetric laminar interacting boundary layers

A. KLUWICK (WIEN)

THE COMPUTATION of high Reynolds number laminar viscous inviscid interaction phenomena has been one of the central issues in fluid mechanics over the past two decades. An important contribution to the understanding of such flows has been provided by asymptotic theories. In particular these theories show that a locally interacting laminar boundary layer develops a multilayer structure. Viscous effects are of importance only inside a thin region adjacent to the wall where the flow is governed by the boundary layer equations, the pressure being coupled to the displacement thickness. Owing to the complicated general form of the pressure-displacement relationship most studies of local interaction processes deal with the case of two-dimensional flow. Three-dimensional interaction effects can be investigated more easily, however, if it is possible to exploit symmetry properties as in the case of axisymmetric flow.

1. Introduction

IT IS ONE of the main goals of modern fluid dynamics to improve the understanding of high Reynolds number internal and external flows. Due to the combination of highly developed computing techniques and powerful analytical methods remarkable progress has been achieved during the past 20 years as far as the case of laminar two-dimensional flow is concerned. Numerical codes based either on the full Navier–Stokes equations or the simplified equations of interacting boundary-layer theory/triple-deck theory are available to calculate such flows including small recirculation regions. Although it is certainly true that difficulties arise in studies dealing with longer separation bubbles and, furthermore, that the transition from weakly to grossly separated flow is not fully understood, still a fairly complete picture of two-dimensional laminar high Reynolds number flows has emerged. In contrast, three-dimensional laminar flows appear to have received much less attention even for weakly separated flows. Within the framework of triple-deck theory SMITH, SYKES and BRIGHTON [44] have studied two-dimensional boundary layers subjected to three-dimensional disturbances. Due to the complicated form of the interaction equations only the linear response of these equations was calculated, thus excluding the possibility of flow separation. Although nonlinear solutions to related types of problems have been obtained by SYKES [59] and more recently by DUCK and BURGGRAF [12], the possibility of treating fully three-dimensional flows appears to be rather limited at present. In order to gain some insight into the basic three-dimensional effects it seems reasonable, therefore, to concentrate on flows exhibiting symmetries which simplify the calculations.

Two classes of such flows have been investigated intensively in the past. The first class concerns swept wing configurations which vary slowly in the spanwise direction. As a consequence the lateral pressure gradient is small and the interaction process is essentially two-dimensional in planes normal to the leading edge of the wing. Interesting phenomena, such as open separation, can therefore be studied with a minimum of computational effort, GITTLER and KLUWICK [16].

Considerable simplifications of the governing equations are also possible if the flow under consideration is axisymmetric. Certainly this assumption appears to be rather re-

strictive at first sight. Still, flows of this type are useful in studying the influence of the three-dimensional spreading of streamtubes on interaction processes, which is also thought to play an important role under more general situations. Most important, it is found that due to this effect the flow near the trailing tip of an axisymmetric body differs substantially from its two-dimensional counterpart. Finally, studies of flows past axisymmetric bodies at incidence have shed some light on the phenomenon of cross-flow separation and the formation of vortex sheets which are important ingredients of three-dimensional separated flows.

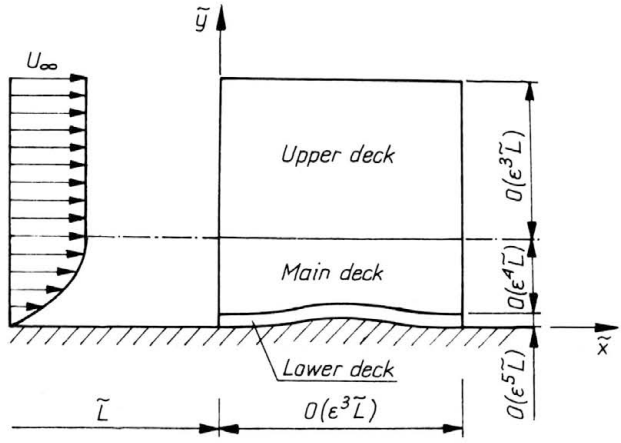

FIG. 1. Triple-deck structure of the interaction region for two-dimensional flow.

2. Triple-deck solutions

As a starting point, some properties of the interaction region holding in the case of strictly two-dimensional flow, Fig. 1, will be briefly summarized. To this end we consider the laminar boundary layer on a flat plate at a distance $\tilde{L}$ from the leading edge which is subjected to disturbances caused, for example, by an impinging shock or a surface mounted obstacle. It is well known then that interaction effects are of importance inside a short region with streamwise extent of $O(\varepsilon^3\tilde{L})$ where

$$\varepsilon = \mathrm{Re}^{-1/8} \ll 1, \quad \mathrm{Re} = \frac{\tilde{U}_\infty \tilde{L}}{\tilde{\nu}_\infty}$$

and Re, $\tilde{U}_\infty$ and $\tilde{\nu}_\infty$ denote the Reynolds number, the free stream velocity and the kinematic viscosity evaluated at free stream conditions, respectively. Outside the boundary layer, in the upper deck region, the perturbations of the field quantities are governed by the linearized equations of inviscid theory. The role played by the main deck, which comprises most of the boundary layer, is a passive one; to transfer displacement effects exerted by the viscous near-wall region—termed the lower deck—to the upper deck and to transfer the resulting pressure disturbances back to the lower deck. Here the flow is governed by the boundary layer equations for an incompressible fluid which can be written

in the form

$$\frac{\partial u}{\partial x}+\frac{\partial v}{\partial y}=0, \quad u\frac{\partial u}{\partial x}+v\frac{\partial u}{\partial y}=-\frac{dp}{dx}+\frac{\partial^2 u}{\partial y^2},$$
$$u=v=0 \text{ on } y=F(x), \tag{2.1}$$
$$u=y \text{ for } x\to-\infty,$$
$$u=y+A(x) \text{ for } y\to\infty,$$

where x, y, u, v and p denote Cartesian coordinates parallel and normal to the free stream direction, the associated velocity components and the pressure, suitably nondimensionalized and rescaled.

The solution to the boundary-layer equations has to satisfy to no-slip condition at the wall which, using a Prandtl transformation, can be applied at $y = 0$. Additional conditions follow from the requirement that the disturbances decay far upstream and from the match between the result holding in the upper, main and lower decks, respectively. The quantity $A(x)$ can be interpreted as a perturbation displacement thickness and thus determines the pressure disturbances via the relationships

$$p(x)=-\frac{1}{\pi}\int_{-\infty}^{\infty}\frac{A'(\xi)}{\xi-x}d\xi \tag{2.2}_1$$

or

$$p(x)=-A'(x) \tag{2.2}_2$$

depending on whether the external flow is subsonic or supersonic. Triple-deck equations of the form (2.1), (2.2), apart from minor changes of the boundary conditions, can be shown to cover a large variety of two-dimensional problems including trailing edge flows, supersonic free interactions, flows with blowing or suction, etc. Many of these applications have been reviewed by STEWARTSON [54], NEILAND [33], SMITH [48], MESSITER [30] and KLUWICK [19].

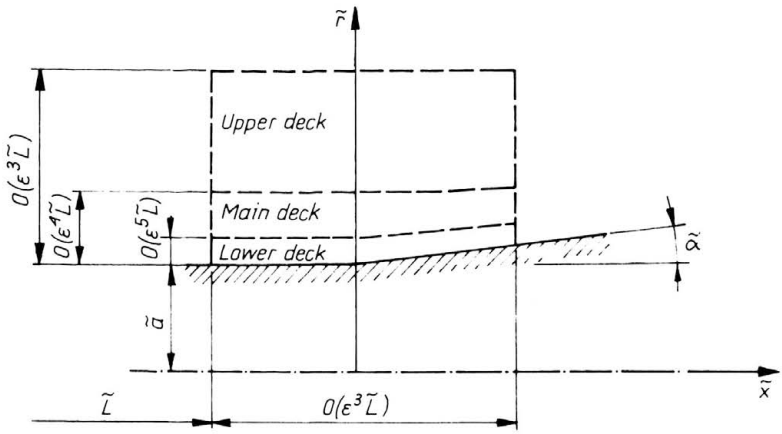

FIG. 2. Triple-deck structure of the interaction region for axisymmetric flow.

Axisymmetric interacting boundary layers have been investigated first by HORTON [18] and VATSA & WERLE [62], and using the triple-deck concept by KLUWICK, GITTER & BODONYI [21], DUCK [11] and TIOMSHIN [60, 61]. As an example of this type of problem the flow past a flared cylinder is sketched in Fig. 2. It will be assumed first that the radius $\tilde{a}$ of the cylinder is of the same order of magnitude as the length of the interaction region in the case of two-dimensional flow $\tilde{a}/\tilde{L} = O(\varepsilon^3)$. Owing to this assumption the thickness of the lower-deck is small compared to $\tilde{a}$ and, as a consequence, the flow inside the viscous layer adjacent to the wall is governed by Eqs. (2.1). Similarly, axisymmetric effects do not affect the flow inside the main deck to leading order. They do, however, have to be taken into account in the upper deck, where they cause modifications of the pressure- displacement relationships. Introducing the scaled cylinder radius

$$a = C^{-3/8}\lambda^{4/5}|1 - M_\infty^2|^{1/8}\left(\frac{\tilde{T}_w}{\tilde{T}_\infty}\right)^{-3/2}\frac{\tilde{a}}{\varepsilon^3\tilde{L}}, \quad \lambda = 0.33206\ldots, \tag{2.3}$$

where M, $\tilde{T}$ and C denote the Mach number, the temperature and the Chapman constant entering the linear viscosity law $\tilde{\mu}/\tilde{\mu}_\infty = C\tilde{T}/\tilde{T}_\infty$, while indices ∞ and w refer to free stream and wall conditions, respectively, and with the Fourier transforms $\overline{p}$, $\overline{A}$, of $p(x)$, $A(x)$, the appropriate viscous inviscid coupling condition for subsonic flow is

$$\begin{aligned} \overline{p}(\omega) &= -i\omega\overline{A}(\omega)H_0^{(1)}(i\omega a)H_1^{(1)}(i\omega a), \quad \mathrm{Re}\,\omega > 0, \\ \overline{p}(\omega) &= -i\omega\overline{A}(\omega)H_0^{(2)}(i\omega a)H_1^{(2)}(i\omega a), \quad \mathrm{Re}\,\omega < 0. \end{aligned} \tag{2.4}_1$$

If the external flow is supersonic, $(2.2)_2$ has to be replaced by

$$p(x) = -A'(x) + \frac{1}{a}\int_{-\infty}^{x} W\left(\frac{x-\xi}{a}\right)A'(\xi)d\xi,$$

$$W(z) = \int_0^z \frac{e^{-\lambda z}}{K_1^2(\lambda) + \pi^2 I_1^2(\lambda)}\frac{d\lambda}{\lambda}. \tag{2.4}_2$$

Note that as $a \to \infty$ $(2.4)_1$ and $(2.4)_2$ reduce to the limiting forms $(2.2)_1$, $(2.2)_2$.

As the scaled body radius tends to zero, $a \to 0$, both $(2.4)_1$ and $(2.4)_2$ yield

$$p(x) = A''(x)a\log a. \tag{2.5}$$

In agreement with the results following from slender body theory, the induced pressure disturbances are proportional to the curvature of the displacement body independent whether the external flow is subsonic or supersonic. In passing we note that the pressure/displacement-relationship (2.5) is similar to that encountered in jets, SMITH & DUCK [43].

While axisymmetric effects are confined to the external flow region, if $a = O(1)$ they eventually penetrate into the boundary layer as $a \to 0$. As pointed out by DUCK [11] two cases, $a = O(\mathrm{Re}^{-1/2})$ and $a = o(\mathrm{Re}^{-1/2})$ leading to interaction length scales of $O(\mathrm{Re}^{-3/7}(\ln \mathrm{Re}))$ and $O(\mathrm{Re}^{-3/6}(\ln \mathrm{Re}))$, respectively, have to be treated separately. The main difference between these regimes is the double structure of the unperturbed boundary layer which develops if the radius of the cylinder is considerably smaller than the classical boundary layer thickness is shown by GLAUERT & LIGHTHILL [14], STEWARTSON [50], BUSH [6]. In both of these cases, however, the effects of curvature are found to modify the flow properties inside the main deck only. To leading order, no

matter how small a is, the governing equations for the viscous wall layer reduce to the two-dimensional boundary layer equations (2.1) supplemented by the pressure-displacement relationship (2.5). As a consequence, Eqs. (2.1) with $(2.4)_1$ or $(2.4)_2$ depending on whether the external flow is subsonic or supersonic provide a consistent description of viscous-inviscid interactions on axisymmetric bodies for arbitrary values of a.

Solutions to the interaction equations for supersonic external flow have been obtained by KLUWICK *et al.* [22, 23] and GITTLER & KLUWICK [15]. In order to gain some insight into the effects caused by the additional integral term of Eq. $(2.4)_2$ as compared to the case of planar flow, it is useful to consider the pressure distribution on a flared cylinder according to inviscid theory, Fig. 3. In the vicinity of the corner the flow is approximately two-dimensional and the pressure jump at the corner can be calculated from the Ackeret relationship. Further downstream, however, the increase of the cross-sectional area of streamtubes due to the axisymmetry of the flow field becomes important and the pressure disturbances thus decrease (to leading order they even vanish in the limit $x = \infty$). This is the well known phenomenon of overcompression/overexpansion which occurs on axisymmetric bodies with concave/convex corners.

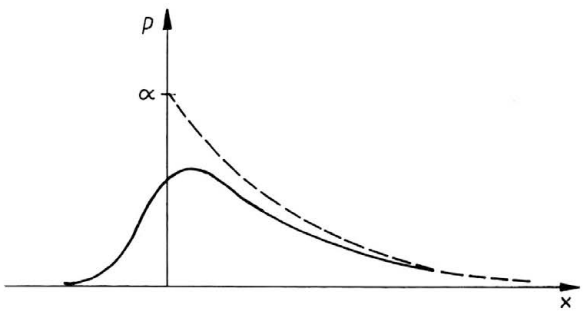

FIG. 3. Pressure distribution an a flared cylinder - - - inviscid flow, — viscous flow.

If viscous effects are taken into account, pressure disturbances make themselves felt well upstream of the corner and, consequently, the magnitude of the pressure peak decreases. One therefore expects that separation on axisymmetric compression ramps, $\tilde{\alpha}^* > 0$, will be delayed as compared to the case of two-dimensional flow and this is confirmed by the numerical results shown in Fig. 4. For sufficiently small values of the scaled ramp angle

$$\tilde{\alpha}^* = \varepsilon^2 \lambda^{1/2} C^{1/4} (M_\infty^2 - 1)^{1/4} \alpha \tag{2.6}$$

the boundary layer remains attached and due to the fact that the numerical computations were carried out for a slightly rounded rather than a perfectly sharp corner, the wall shear stress assumes its minimum value upstream of $x = 0$. As α increases, the minimum of the wall shear stress distribution decreases and incipient separation occurs at $\alpha_{is} \approx 3.39$ ($a = 1$) which should be compared with the corresponding result holding in the case of planar flow $\alpha_{is} \approx 1.57$ ($a = \infty$) obtained by RIZZETTA, BURGGRAF & JENSON [37]. For larger values of α the boundary layer separates upstream of the corner and reattaches at the cone surface. As expected, the pressure increase near the reattachment point is smaller than in the case of two-dimensional flow. Moreover, the maximum of the pressure distribution differs only slightly from the value of the pressure disturbance at the reattachment point

and the compression region upstream of this point is followed by a zone of rapid expansion caused by the increasing stream tube area. Finally, it should be noted that the formation of a plateau region of almost constant pressure for large values of α is clearly visible in Fig. 4.

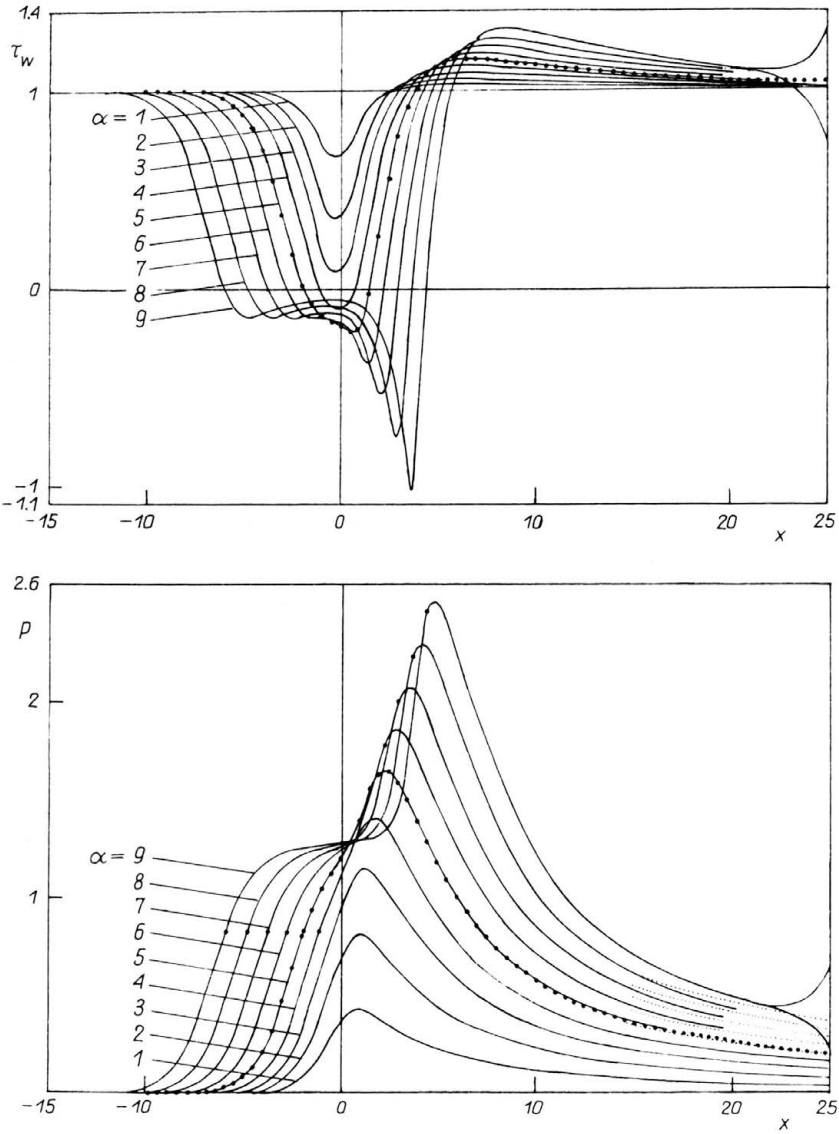

FIG. 4. Pressure and wall-shear stress distributions for $a = 1$ and various positive cone angles α (GITTLER and KLUWICK [15]).

The structure of the flow inside the plateau region is sketched in Fig. 5. Similar to the case of planar flow the fluid is slowly moving upstream in the main part of this region. To leading order viscous effects are of importance only inside a thin boundary layer adjacent to the wall where the no slip condition has to be satisfied and inside a thin shear layer

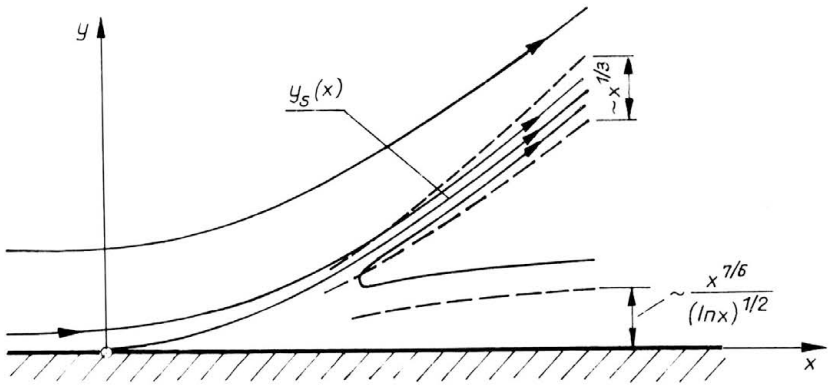

FIG. 5. Asymptotic structure of the plateau region.

centered at the separation streamline. However, while in the case of two-dimensional flow the perturbation displacement thickness is a linear function of the distance x from the separation point, such a linear thickening of the displacement body is not sufficient to generate an axisymmetric separated flow region of constant pressure. Inversion of Eq. $(2.4)_2$ with $p = p_o = \text{const}$ yields, KLUWICK *et al.* [22]

$$A(x) \sim \frac{p_0}{a}\left[\frac{x^2}{2\ln x} + \frac{x^2}{(\ln x)^2}\left(\frac{3}{4} + \frac{1}{2}\ln\frac{a}{2}\right)\right] \quad \text{as} \quad x \to \infty. \tag{2.7}$$

It should be noted that the derivation of Eq. (2.7) requires that $x/a >> 1$ and thus the above expression does not reduce to the two-dimensional result $A(x) \sim -p_0 x$ as $a \to \infty$. To recover the two-dimensional case it would be necessary to carry out the limit $a \to \infty$ with $x \gg 1$ fixed.

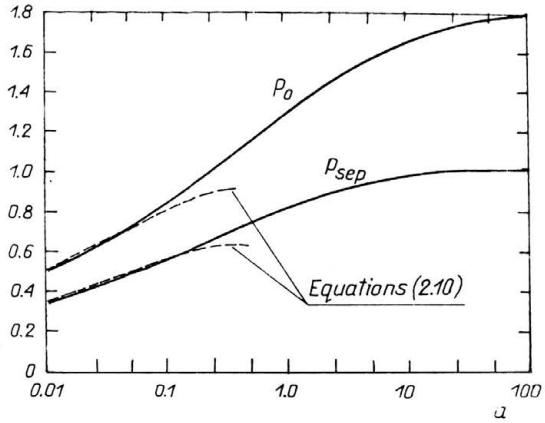

FIG. 6. Variation of the plateau pressure p_0 and the value of the pressure at separation p_{sep} with a.

The variation of the plateau pressure, p_0, and the separation pressure, p_{sep}, with a is depicted in Fig. 6. It is seen that both p_0 and p_{sep} assume their largest values in the case of two-dimensional flow $a \to \infty$ while they tend to zero in the limit $a \to 0$. To study the

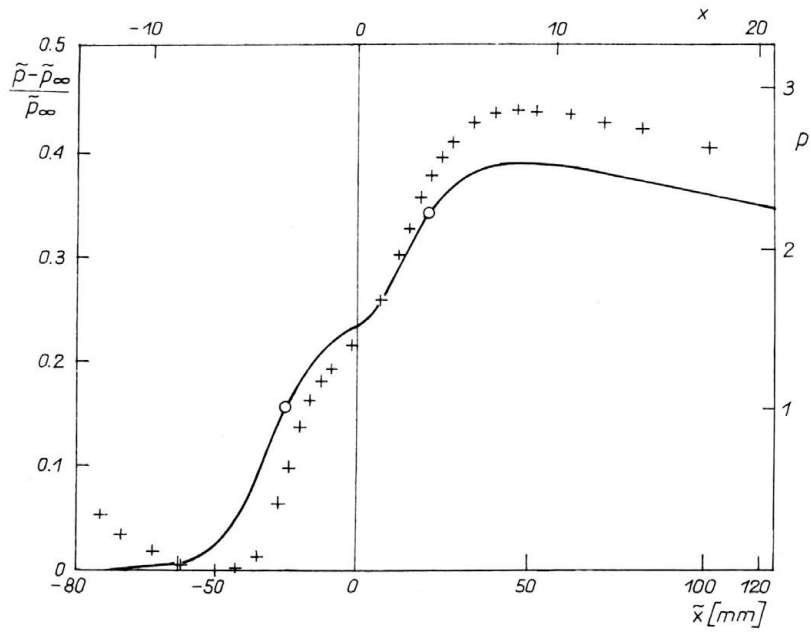

FIG. 7. Comparison between experimental and theoretical results: +++, experimental data from LEBLANC and GINOUX ([25], Fig. 4a); $M_\infty = 2.25$, $Re = 8.7 \cdot 10^4$, $\alpha^* = 7.5°$, $a = 34.6$; — triple deck solution (KLUWICK *et al.* [21]).

properties of p_0 and p_{sep} for $a \to 0$ it is convenient to introduce the transformation

$$\begin{aligned} x &= (-a \ln a)^{3/7} x^*, \quad y &&= (-a \ln a)^{1/7} y^*, \\ u &= (-a \ln a)^{1/7} u^*, \quad v &&= (-a \ln a)^{-1/7} v^*, \\ A &= (-a \ln a)^{1/7} A^*, \quad p &&= (-a \ln a)^{2/7} p^*, \end{aligned} \tag{2.8}$$

which leaves equations (2.1) unchanged while the pressure-displacement relationship (2.5) reduces to

$$p^* = -d^2 A^*/dx^{*2}. \tag{2.9}$$

As mentioned earlier, interaction problems of exactly this form have been studied in a different context by SMITH & DUCK [43] and by SMITH & MERKIN [48]. Combination of their numerical results $p_0^* = 1.222$, $p_{sep}^* = 0.855$ and (2.8) yields the dependence of the plateau pressure and the separation pressure on a in the limit $a \to 0$

$$p_0 \sim 1.222(-a \ln a)^{2/7}, \quad p_{sep} \sim 0.855(-a \ln a)^{2/7}. \tag{2.10}$$

In Fig. 7 one set of experimental data obtained by LEBLANC & GINOUX [25] in the 16 in. × 16 in. continuous supersonic wind tunnel of the von Kármán Institute is compared with a numerical solution of the triple-deck equations (2.1), $(2.4)_2$. The test conditions correspond to adiabatic flow over a flared cylinder with $\tilde{\alpha} = 7.5°$ at $M_\infty = 2.25$ with $Re = 8.7 \times 10^4$ and $a = 34.6$. As in the case of two-dimensional flow investigated by RIZZETTA *et al.* [37], the initial pressure rise in the interaction region is overpredicted by the asymptotic theory. In addition, inspection of Fig. 7 shows that the pressure maximum is lower than the value determined experimentally by about 11%. This discrepancy seems to be caused mainly by the linearization of the governing equations in the upper deck.

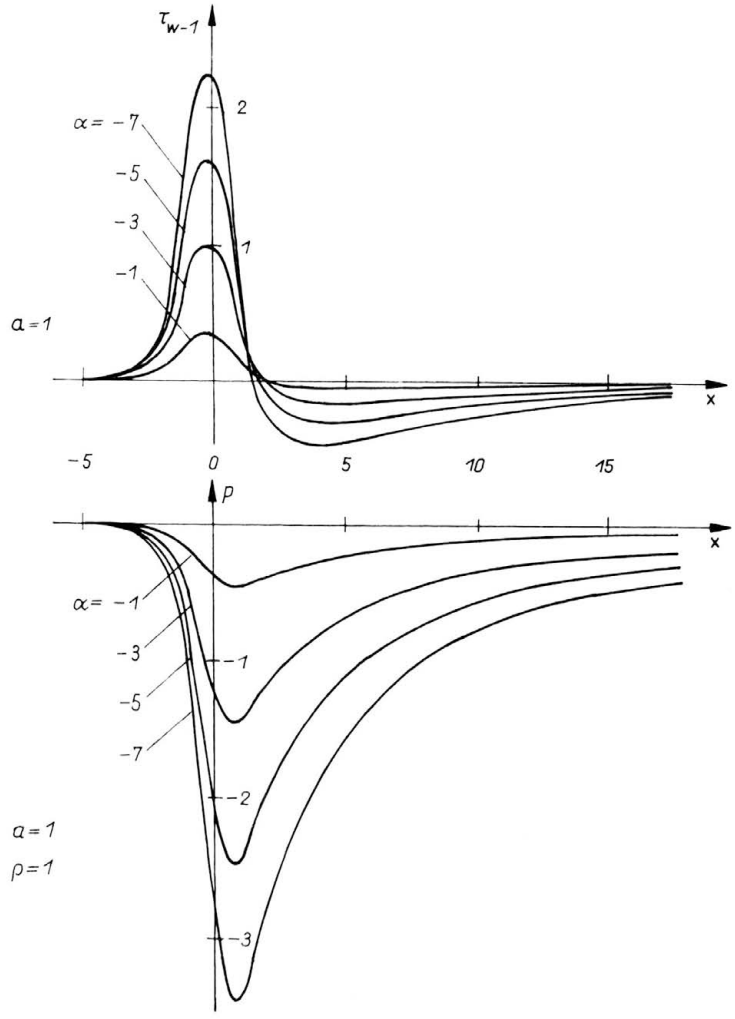

FIG. 8. Pressure and wall shear stress distribution for $a = 1$ and various negative cone angles α (GITTLER and KLUWICK [15]).

Some numerical results for negative flare angles (convex corners) are summarized in Fig. 8. Owing to the pressure drop upstream of the corner the wall stress increases initially. The formation of a recompression zone downstream of the corner, however, causes the wall shear stress to decrease before it finally rises again to approach the unperturbed value $\tau_w = 1$ far downstream. Furthermore, the minimum of the wall shear stress distribution is seen to drop progressively as the flare angle $(-\alpha)$ increases indicating the possibility of boundary layer separation if $(-\alpha)$ is sufficiently large which was confirmed numerically. Since this effect is a direct consequence of the overexpansion and subsequent recompression of the fluid as it turns around the corner, it does not occur in the case of two-dimensional expansion ramps where the flow remains attached for all values of $-\alpha \geq 0$.

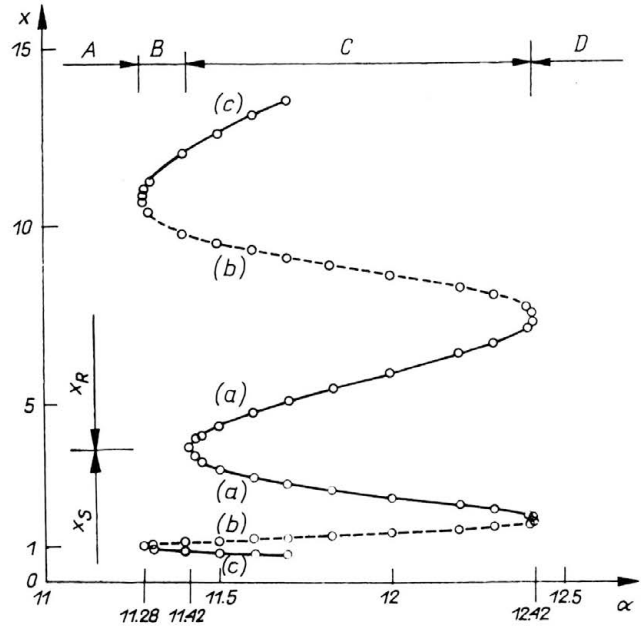

FIG. 9. Variation of x_S and x_R with α for $a = 1$ (GITTLER and KLUWICK [15]).

In Fig. 9 the position of the separation and the reattachement points is plotted as function of the flare angle, α, for $a = 1$. If $\alpha \geq -11.28$ the boundary layer remains attached and the solutions of the interaction problem are unique. In contrast, two solutions exhibiting relatively long separated flow regions and a third one yielding attached flow are obtained if $-11.42 \leq \alpha \leq -11.28$. For values of the turning angle $\alpha < -11.42$ attached flow is no longer possible. The numerical results point to the existence of three different types of separated flow within the range $-11.42 < \alpha < -12.42$ and, furthermore, indicate that the triple-deck solutions are again unique if $\alpha < -12.42$. Unfortunately, the numerical scheme used by GITTLER & KLUWICK [15] did not yield converged solutions with long recirculation zones for $\alpha < -11.7$. This difficulty may be caused by the FLARE approximation which was employed to prevent numerical instabilities once flow reversal occurs. However, as pointed out in a recent study by SMITH [49], it seems to be a common feature encountered in all the computational methods to date that "the computations become increasingly difficult/numerically unstable as the reversed-flow eddy strengthens". Therefore, the possibility that the triple deck equations cease to be valid if $-\alpha$ exceeds a finite critical value should be considered too. Indeed, it has been shown by SMITH [49] that a structure describing a reversed-flow singularity can be derived from all forms of the interaction equations known to date.

Figure 10 shows the pressure and wall-shear-stress distributions for $a = 1$ and $\alpha = -11.6$ corresponding to the three different branches depicted in Fig. 9. While the results for the solution with a short separation bubble are qualitatively similar to those for attached flow, the two solutions with longer recirculation zones exhibit interesting new features. Most important, it is seen that the shape of the pressure and wall-shear stress

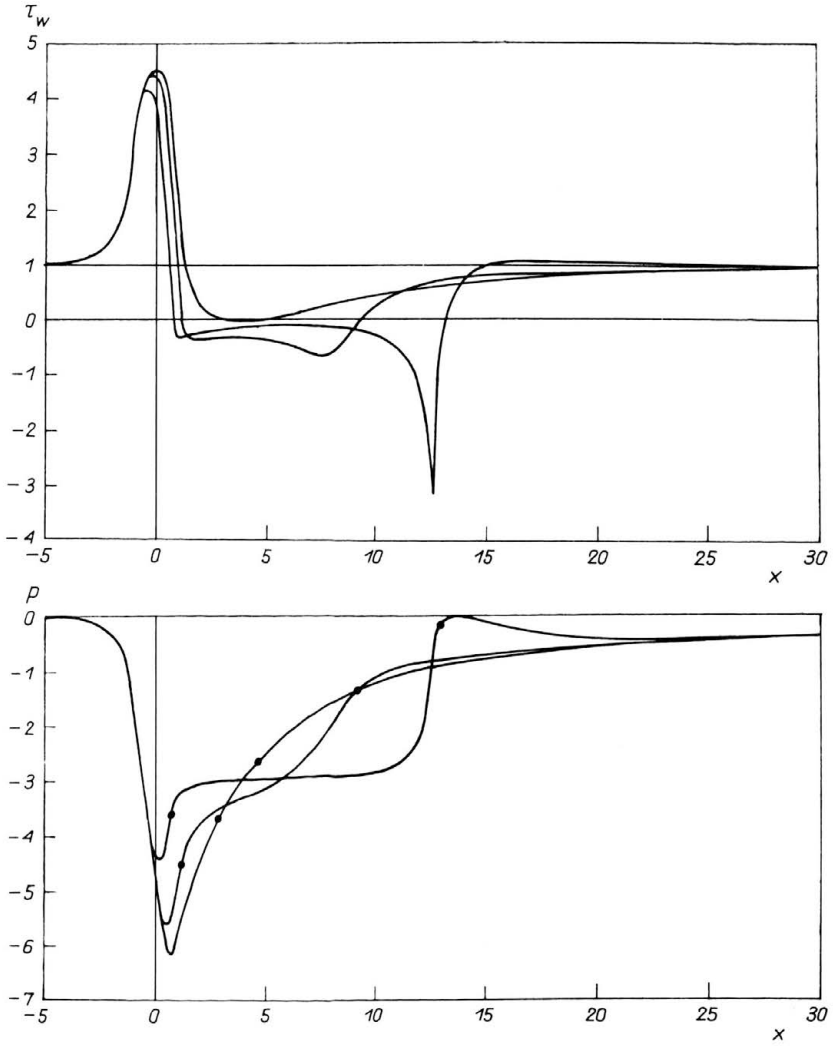

FIG. 10. Pressure- and wall-shear stress distributions for $\alpha = 1$ and $\alpha = -11.6$ (GITTLER and KLUWICK [15]).

distributions downstream of the separation points now qualitatively resemble those for separated flows over flared cylinders with $\alpha > 0$ depicted in Fig. 4. in spite of the fact that the pressure disturbances within the recirculation zones are negative. In particular, the formation of a plateau region with $p_0 < 0$ in the solution with long separation bubble is clearly visible in Fig. 10.

3. Marginal separation

The results depicted in Fig. 10 show that a supersonic laminar boundary layer may separate downstream of an axisymmetric expansion ramp if the turning angle $-\alpha$ of the flow is sufficiently large. In contrast, investigations by STEWARTSON [52, 53] and others

indicate that the boundary layer remains attached in the case of planar flow even in the limit $|\alpha| \to \infty$. This raises the question how this transition takes place as the scaled body radius a tends to infinity in the pressure-displacement relationship $(2.4)_2$. No detailed numerical investigation dealing with this problem has been carried out so far. Preliminary results by GITTLER (private communication) indicate that the point of zero wall-shear stress at incipient separation moves downstream as a increases. This suggests that the position of the separation point eventually leaves the triple-deck scaling and that separation will then be caused by an imposed rather than a self-induced pressure gradient. As a consequence, a Goldstein singularity may be expected to form at the separation point. However, since the boundary layer remains attached in the case of strictly two-dimensional flow this singularity will be weak for a certain combination of values a and $|\alpha|$.

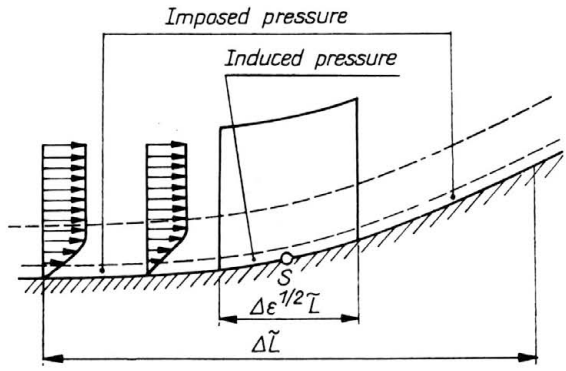

FIG. 11. Asymptotic flow structure for $\mathrm{Re}^{-3/8} \ll \Delta$.

Similar considerations hold in the case of smoothed axisymmetric compression/expansion ramps if the distance $\Delta\tilde{L}$ over which the transition from the cylindrical to the conical geometry takes place is large compared to the triple-deck length scale. Figure 11 shows the asymptotic structure of the resulting flow field which has been investigated by KLUWICK [20] under the assumption that $\Delta\tilde{L}$ is still small compared to the typical boundary-layer length scale: $\mathrm{Re}^{-3/8} \ll \Delta \ll 1$. As a consequence, viscous effects on the disturbances caused by the ramp are negligible small over most of the boundary-layer and have to be taken into account only in a thin region adjacent to the wall. The requirement that (i) axisymmetric effects are retained in the equations governing the flow outside the boundary layer and that (ii) acceleration, pressure gradient and viscous terms are equally important inside the viscous sublayer leads to the following estimates for the thickness $H\tilde{L}$ of this sublayer, the ramp angle $\tilde{\alpha}$, and the cylinder radius $a\tilde{L}$ in terms of Δ:

$$H = O(\Delta^{1/3}\mathrm{Re}^{-1/2}), \quad \tilde{\alpha} = O(\Delta^{2/3}), \quad a = O(\Delta). \tag{3.1}$$

Introducing appropriate asymptotic expansions based on these estimates one recovers the boundary-layer equations (2.1). In contrast to the triple-deck problem, however, the lateral displacement of the external inviscid flow caused by the viscous sublayer is too small to influence the leading order term of the expansion of the pressure disturbances. In the

case of external supersonic flow Eq. $(2.4)_2$ has to be replaced by

$$p = -R_w'(x) + \frac{1}{a}\int_{-\infty}^{x} W\left(\frac{x-\xi}{a}\right) R_w'(\xi)d\xi, \tag{3.2}$$

where $R_w(x)$ characterizes the (scaled) distance of the body surface from its unperturbed position far upstream. The flow inside the boundary layer thus is seen to be driven by an imposed pressure gradient. In general, this will lead to the occurrence of a Goldstein singularity at the point of vanishing skin friction which terminates the integration of Eqs. (2.1), (3.2). However, as shown by RUBAN [40] there exists yet another type of a singular solution that can be extended continuously through a point of zero skin friction. Let α_c denote the value of α at incipient separation, then the wall shear stress distribution associated with this solution is given by

$$\alpha = \alpha_c : \frac{\partial u}{\partial y}|_{y=0} \sim a_0|x - x_s|, \quad x \to x_s. \tag{3.3}$$

Here a_0 and x_s denote a positive constant and the position of the point of vanishing skin friction, respectively. Equation (3.3) is a special case of the more general relationship

$$\begin{aligned} |\alpha| &= |\alpha_c| + k\varepsilon, \\ \frac{\partial u}{\partial y}|_{y=0} &\sim a_0\sqrt{(x-x_s)^2 - a_1^2 k\varepsilon}, \\ |k| = O(1), \quad |a_1| &= O(1), \quad \varepsilon \ll 1, \end{aligned} \tag{3.4}$$

holding for $|\alpha - \alpha_c| \ll 1$. According to this relationship $(\partial u/\partial y)_{y=0} > 0$ in the vicinity of the point $x = x_s$ if $|\alpha| < |\alpha_c|$ while the wall shear stress distribution exhibits a weak Goldstein singularity at $x = x_s - \sqrt{a_1^2 k\varepsilon}$ if $|\alpha| > |\alpha_c|$. Since the singular behaviour of the wall shear stress is accompanied by a singularity of the vertical velocity component as well, Eq. (3.2) expressing the result that the displacement thickness does not influence the pressure disturbances to leading order is violated locally. This suggests that a local interaction theory can be formulated which describes the flow properties near $x = x_s$ and indeed it can, RUBAN [41], STEWARTSON, SMITH & KAUPS [55].

Order of magnitude estimates similar to those leading to Eq. (3.1) indicate that the streamwise and lateral extent of the interaction region is $O(\varepsilon^{1/2})$ and the included pressure perturbations enter the governing equations at the appropriate order if

$$\varepsilon^{1/2} = O(\Delta^{-8/15}\,\mathrm{Re}^{-2/5}). \tag{3.5}$$

Since the lateral extent of the interaction region is small compared to the characteristic body radius, axisymmetric effects are negligibly small inside the boundary layer as well as in the external flow region. In the viscous sublayer adjacent to the wall the Navier–Stokes equations reduce to the boundary-layer equations (linearized with respect to the separation profile) to first and second order. To determine the first-order approximation of the wall shear stress it is necessary to investigate the properties of the second-order solution at large distance from the wall. Elimination of the exponentially growing term using the pressure-displacement relationship $(2.2)_1$ for two-dimensional subsonic external

flow leads to the integro-differential equation

$$A^2 - \overline{X}^2 + \Gamma = -\int_{\infty}^{\overline{X}} \frac{A''(\xi)}{\sqrt{\xi - \overline{X}}}\, d\xi \tag{3.6}$$

for the (scaled) wall shear stress A in terms of the (scaled) streamwise coordinates $\overline{X} \propto (x - x_s)/\varepsilon^{1/2}$. Here $\Gamma \propto (|\alpha| - |\alpha_c|)/\varepsilon$ characterizes the difference between the actual value of the ramp angle and α_c.

It can be shown that (3.6) also controls marginal separation in the case of supersonic flow. To this end it is necessary to modify the definitions of the scaled variables such that the sign of $\overline{X}$ is changed. As a consequence, separation/reattachement in subsonic flow corresponds to reattachement/separation in supersonic flow.

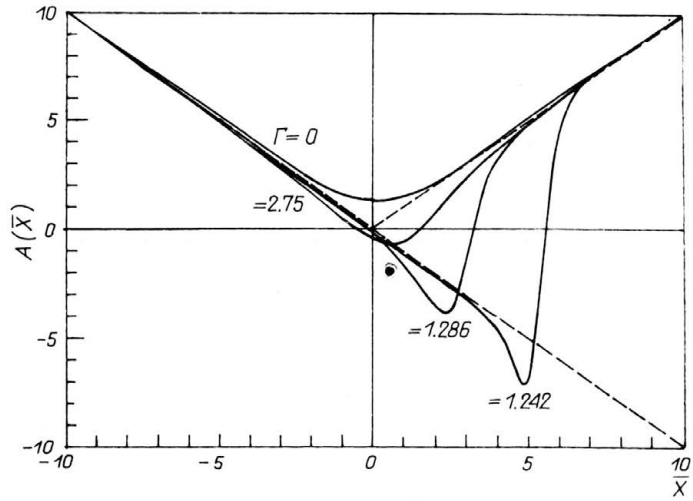

FIG. 12. Wall shear stress distribution for various values of the scaled turning angle Γ.

Numerical solutions of (3.6) for various values of the parameter Γ assuming incompressible flow have been obtained by RUBAN [41], STEWARTSON *et al.* [55] and BROWN & STEWARTSON [5]. Some results for $\Gamma > 0$ corresponding to values of the ramp angle $|\alpha|$ which exceed the critical value $|\alpha_c|$, leading to marginal separation according to classical boundary-layer theory, are depicted in Fig. 12. It is seen that separation is delayed by the interaction between the boundary layer and the external inviscid flow. Furthermore, the results show that the wall shear stress distributions are almost symmetrical with respect to the origin $\overline{X} = 0$ if the boundary layer is fully attached or contains a small separation bubble. As the length of the separation bubble increases, however, the minimum of the wall shear stress is shifted downstream. In the case of very long separation bubbles interaction effects are of importance mainly in the vicinity of the reattachement point where a rapid transition from the local solution for regular boundary-layer separation $A = -\overline{X}$ to the local solution controlling marginal separation $A = \overline{X}$ takes place.

Figure 13 displays the variation of the position $\overline{X}_s/\overline{X}_R$ of the separation/reattachement point with Γ. If $\Gamma < 0$ the boundary layer remains fully attached and the solutions to the interaction equations (3.6) are unique. If $\Gamma > 0$, however, two or four different solutions

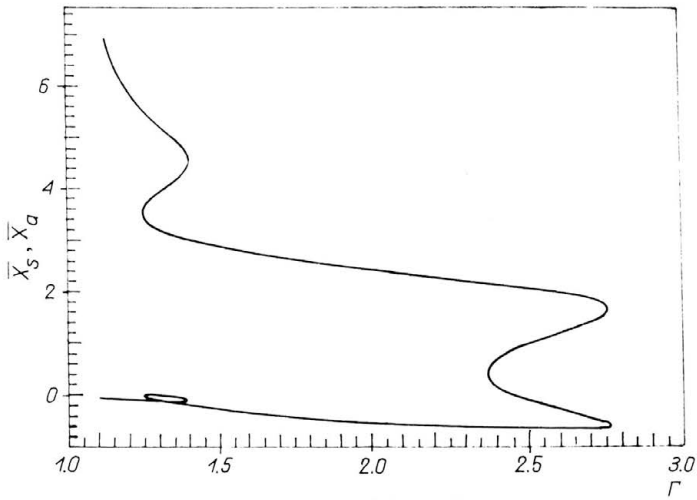

FIG. 13. Variation of $\overline{X}_S$ and $\overline{X}_R$ with Γ.

can be calculated in the parameter range $0 \leq \Gamma < \Gamma_c$ while solutions cease to exist for $\Gamma > \Gamma_c$ where $\Gamma_c \approx 2.75$. The nonexistence of solutions for large positive values of Γ indicates that a substantial change of just marginally separated flow, possibly leading to global separation, must occur as Γ increases beyond the critical value Γ_c. However, it is not known yet how this transition takes place.

4. Trailing-tip flows

In all cases considered so far the thickness of the viscous sublayer of the local interaction region was found to be small compared to the characteristic body radius. As a consequence the flow close to the wall was governed by the two-dimensional form of the boundary layer equations and axisymmetric effects were of importance only insofar as they changed the pressure displacement relationship. However, there are many real applications where such a description of the interaction process no longer applies and an important one is the trailing-tip region of an axisymmetric body of finite length.

In contrast to the case of two-dimensional flow near the trailing tip of a flat plate which has been studied in detail starting with the pioneering work of STEWARTSON [51] and MESSITER [29], trailing-tip flows have received much less attention. A summary of studies dealing with such flows has been given by BODONYI, SMITH & KLUWICK [3] who investigated the local flow structure assuming that the body under consideration is so slender that the effect of the pressure gradient on the evolution of the boundary layer according to classical theory can be neglected. The boundary-layer equations can then be written in the form

$$\begin{aligned} &\frac{\partial}{\partial x}(ru) + \frac{\partial}{\partial r}(rv) = 0, \\ &u\frac{\partial u}{\partial x} + v\frac{\partial u}{\partial r} = \frac{\partial^2 u}{\partial r^2} + \frac{1}{r}\frac{\partial u}{\partial r}. \end{aligned} \tag{4.1}$$

Here (u, v) denote the non-dimensional velocity components of an incompressible viscous fluid in a cylindrical coordinate system (x, r), Fig. 14. Coordinates and velocity compo-

nents are nondimensionalized with the length $\tilde{L}$ of the body and the freestream velocity $\tilde{U}_\infty$, respectively. In addition, r and v are scaled with $\mathrm{Re}^{-1/2} = (\tilde{U}_\infty \tilde{L}/\tilde{\nu})^{-1/2}$ in the usual manner.

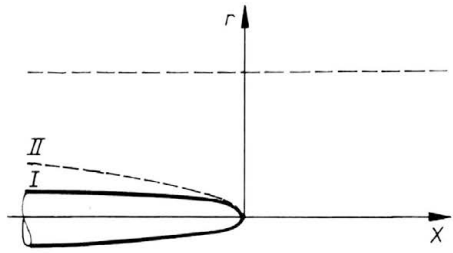

FIG. 14. Multilayer structure of the trailing tip area for $1/4 < n < 1/2$ (BODONYI *et al.* [3]).

The boundary conditions of Eqs. (4.1) include the no-slip condition at the body surface, the symmetry condition at the wake centerline and the requirement that the axial velocity component approaches its freestream value at large distances from the wall:

$$\begin{aligned} &u = v = 0 \quad \text{on} \quad r = r_b(x), \quad 0 \le x \le 1, \\ &v = \frac{\partial u}{\partial r} = 0 \quad \text{on} \quad r = 0, \quad x > 1, \\ &u \to 1 \quad \text{as} \quad r \to \infty. \end{aligned} \tag{4.2}$$

Solutions to Eqs. (4.1), (4.2) have to be calculated numerically in general. To this end BODONYI *et al.* [3] considered body shapes of the form

$$r_b(x) = a(1-x)^n x^{1/2}, \quad 0 \le x \le 1, \tag{4.3}$$

where a is an arbitrary constant. It is perhaps tempting to expect the fluid motion in the trailing tip area of an axisymmetric body to be just a minor generalization of the two-dimensional case. In this latter case the boundary layer is essentially unperturbed upstream of the trailing edge interaction region where the velocity profile undergoes a rapid transition over a distance $O(\mathrm{Re}^{-3/8})$ tending to zero in the limit $\mathrm{Re} \to \infty$. In contrast, the boundary layer on an axisymmetric body is forced to adjust much more gradually, in fact well ahead of the trailing tip interaction region. In this pre-interaction region the evolution of the boundary layer is dominated by the large relative changes of the body radius which grow without bound as the trailing tip is approached. As a consequence one would expect viscous effects to be of importance only within a small fraction of the oncoming classical boundary layer thus leading to the development of an interesting but rather complicated multilayered structure. As shown by BODONYI *et al.* [3] three different ranges of the exponent n characterizing the trailing-tip shape have to be considered.

A scheme of the flow structure for $1/4 < n < 1/2$ is depicted in Fig. 14. In this case viscous effects are confined to a thin layer I comparable in thickness with the body radius $r_b(x)$. Here the stream function ψ can be expressed in terms of the similarity solution

$$\psi(x,r) = Xf(\xi), \quad X = 1-x, \quad \xi = \frac{r}{aX^n}, \tag{4.4}$$

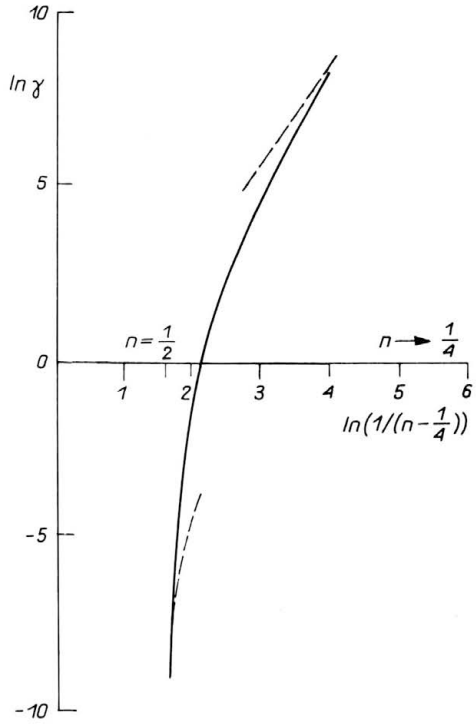

FIG. 15. Variation of the effective wall shear stress $\gamma = f''(1)$ with n for $1/4 < n < 1/2$ (BODONYI *et al.* [3]).

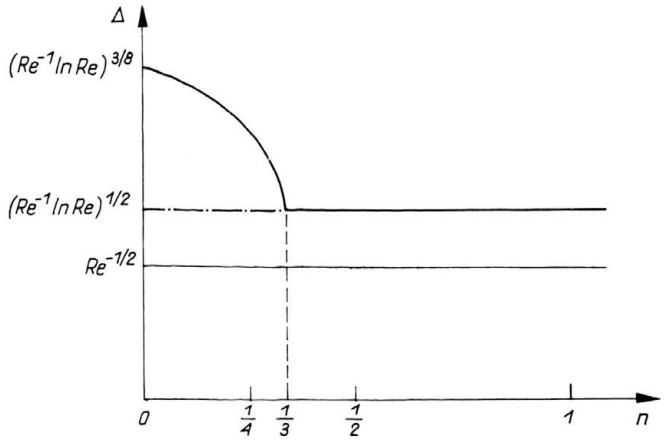

FIG. 16. Variation of the interaction length scale Δ with n (BODONYI *et al.* [3]).

while in Region II outside the viscous sublayer the appriopriate representation of ψ is given by

$$\psi = \psi_0(r) + o(1), \quad r = O(1), \tag{4.5}$$

which describes a slightly perturbed uniform shear flow. The function $\psi_0(r)$ depends on the entire history of the boundary layer upstream of the trailing tip area and cannot be determined by local considerations. Substitution of the relationship (4.4) into Eqs. (4.1), (4.2) yields

$$(2n-1)\xi(f'/\xi)^2 + (f(f'/\xi))' = (\xi(f'/\xi)')', \qquad f(1) = f'(1) = 0, \tag{4.6}$$

where $()'$ denotes differentiation with respect to ξ. A third boundary condition follows from the investigation of the asymptotic behavior of $f(\xi)$ as $\xi \to \infty$. Matching with the solution (4.5) holding outside the viscous sublayer requires that the viscous terms of Eqs. (4.6) vanish at large distances from the wall which leads to

$$f(\xi) \sim B\xi^{1/n}, \quad B > 0 \quad \text{as} \quad \xi \to \infty. \tag{4.7}$$

Equations (4.6), (4.7) have been solved numerically using both shooting and finite difference techniques. The variation of the effective wall shear stress $\gamma = f''(1)$ with n, depicted in Fig. 16, indicates that $\gamma \to 0$ as $n \to 1/2$ while $\gamma \to \infty$ as $n \to 1/4$ which can be confirmed analytically by means of asymptotic expansions. In addition, these analytical results provide useful information how the double structure holding for $1/4 < n < 1/2$ has to be modified if $n < 1/4$ or $n > 1/2$. In both cases the oncoming boundary layer develops a three tiered rather than a two-tiered structure, viscous effects being confined to the innermost layer. However, while the thickness of the viscous sublayer is small compared to the local body radius if $n < 1/2$, this layer is much thicker than X^n if $n > 1/2$. Again it is found that the description of the flow in the outermost region of the boundary layer contains a certain amount of arbitrariness which reflects the influence of the entire flow between the leading and trailing tips. In contrast, the solutions in the thinner layers are determinated uniquely to leading order.

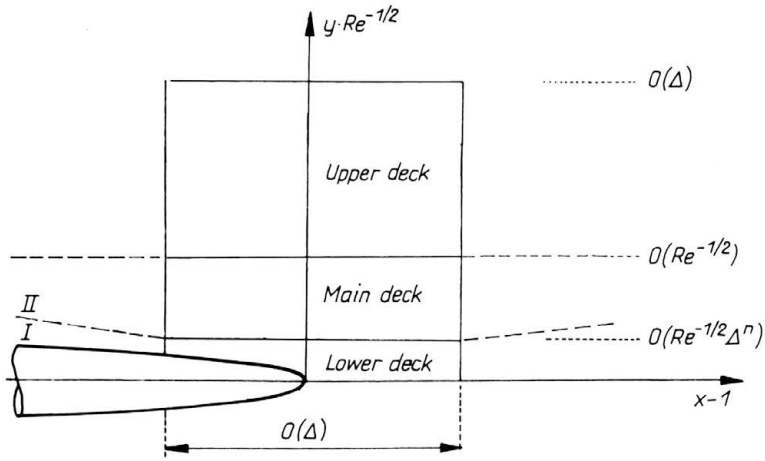

FIG. 17. Asymptotic structure of the trailing tip local interaction region for $1/4 < n < 1/3$.

The results discussed so far are based on the assumption that the pressure gradient term of the boundary-layer equations is negligibly small compared to the inertia and

viscous terms. Owing to the boundary-layer displacement exerted on the external inviscid flow and the resulting pressure response, however, this assumption is violated at very small distances from the trailing tip $X = O(\Delta)$ where viscous inviscid interaction finally comes into play. Application of slender body theory (e.g. COLE [9], pp. 182) yields the order of magnitude estimate

$$p = O(\mathrm{Re}^{-1} \ln \mathrm{Re}) \frac{d^2\delta}{dx^2} \tag{4.8}$$

for the feedback pressure where $\delta(x)$ is a representative displacement function such that $\psi \sim \frac{1}{2}r^2 - \delta(x)$ in Eqs. (4.1), (4.2) as $r \to \infty$ for all x. To determine the interaction length scale Δ the induced pressure gradient has to be compared with the smallest interia term inside the boundary layer. The final results, plotted in Fig. 17, show that Δ depends on the parameter n which characterizes the body shape in the pre-interaction region. It is seen that the interaction length scale is largest in the case of a blunted trailing tip $n = 0$. In this limit Δ is proportional to $\mathrm{Re}^{-3/8}$ but the result holding for planar flow is slightly modified by the occurrence of the $\ln \mathrm{Re}$ term. As n increases, Δ is found to decrease initially but remains constant $\Delta = O(\mathrm{Re}^{-1} \ln \mathrm{Re})^{1/2}$ for $n > 1/3$. As a consequence, the streamwise extent of the trailing tip local interaction region is large compared to the boundary-layer thickness for all values of n.

As pointed our earlier, interaction effects are of importance at distances from the trailing tip where the induced pressure gradient is comparable in magnitude with a representative inertia term inside the boundary layer. Evaluation of the results holding for $n < 1/3$ shows that the inertia terms are smallest inside the viscous sublayer adjacent to the body surface. Therefore, this layer is affected first by the interaction pressure as one would expect from previous triple-deck studies of two-dimensional and three-dimensional flows. In contrast, the feedback pressure first affects the outermost region of the boundary layer if $n > 1/3$. It remains to be clarified whether a more complicated significant interaction is delayed until the length scale $1 - x$ is still smaller.

To complete the description of the flow past a slender axisymmetric body of finite length the trailing tip local interaction region has to be investigated next. Most of this work, however, still remains to be carried out. Results for the case $1/4 < n < 1/3$ have been obtained by BODONYI & KLUWICK [2]. As shown in Fig. 17 the interaction region then comprises a region of external inviscid flow and two wall layers which are the continuation of Regions I and II of the pre-interaction zone. In contrast to the problems considered in Sect. 4, axisymmetric effects are of importance in all three layers of the interaction region but, again, it is possible to express the solutions holding in the upper and the main decks in closed form. The flow inside the lower deck is governed by the axisymmetric form of the boundary-layer equations for an incompressible fluid

$$\begin{aligned} &\frac{\partial}{\partial X}(YU) + \frac{\partial}{\partial Y}(YV) = 0, \\ &U\frac{\partial U}{\partial X} + V\frac{\partial U}{\partial Y} = -\frac{dP}{dX} + \frac{\partial^2 U}{\partial Y^2} + \frac{1}{Y}\frac{\partial U}{\partial Y}, \end{aligned} \tag{4.9}$$

where (X, Y), (U, V) and P denote cylindrical coordinates, the velocity components and the pressure (all suitably scaled), respectively. Equations (4.9) are supplemented with the boundary conditions at the body surface $Y = F(X)$ and the wake center-

line

$$
\begin{aligned}
&U = V = 0 \quad \text{on} \quad Y = F(X), \quad X < 0, \\
&\frac{\partial U}{\partial Y} = V = 0 \quad \text{on} \quad Y = 0, X > 0.
\end{aligned} \tag{4.10}
$$

Consistency with the prescribed body shape in the preinteraction zone requires $F(X) \sim (-X)^n$, $X \to -\infty$.

Finally, matching with the velocity profile in I given by Eqs. (4.4), (4.7) and with the results holding in the main and upper deck yields

$$
\begin{aligned}
U &= \frac{(-X)^{1-n}}{Y} f'\left(\frac{Y}{(-X)^n}\right), && X \to -\infty, \\
U &= KY^{\frac{1-2n}{n}} + \frac{1-2n}{n} KY^{\frac{1-4n}{n}} A(\zeta), && Y \to \infty, \\
K &= B/n, \\
P &= -\frac{1}{2} A''(X).
\end{aligned} \tag{4.11}
$$

The solution of the interaction equations (4.1), (4.10) and (4.11) poses an extremely difficult problem. Numerical calculations have started just recently and no converged results are available at present.

5. Incompressible flow past cones at incidence

Experimental as well as numerical studies dealing with high Reynolds number flows past axisymmetric bodies at incidence have revealed the formation of strikingly complex streamline patterns if boundary layer separation occurs, BIPPES & TUREK [1]. It is not surprising, therefore, that such flows have received scant attention, theoretically, so far. Starting from the pioneering work of LEGENDRE [26], OSWATITSCH [34] and LIGHTHILL [27] a number of interesting new results concerning the local behavior and global topological structure of general three-dimensional separating flows have been obtained by HORNUNG & PERRY [17], PERRY & CHONG [35], DALLMANN [10]. However, attempts to calculate the complete flow field generated by an axisymmetric body at incidence are rare and appear to concentrate mainly on the case of conical tips.

Let (x, r, ϕ) denote cylindrical coordinates with corresponding velocity components (u, v, w) where x, r are nondimensional with the length $\tilde{L}$ of the cone and u, v, w, are nondimensional with the free stream velocity $\tilde{U}_\infty$. Furthermore, let the cone axis coincide with the x-axis. Then the body surface is given by

$$
r = \varepsilon x, \quad 0 \ll \varepsilon \ll 1, \tag{5.1}
$$

where ε denotes the semi-vertex angle of the cone which is assumed to be small and of the same order of magnitude as the angle of incidence $\alpha = \varepsilon\alpha_0$, $\alpha_0 = O(1)$. Introducing the stretched distance from the cone surface $Y = \mathrm{Re}^{1/2}(r - \varepsilon x)$, $\mathrm{Re} = \tilde{U}_\infty \tilde{L}/\tilde{\nu}$, and

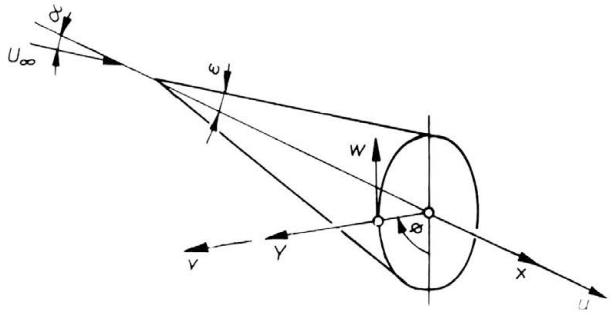

FIG. 18. Flow past a slender cone at a small angle of attack.

asymptotic expansion of the form

$$
\begin{aligned}
u &= u_1(x, Y, \phi) + \ldots, \\
v &= \varepsilon u_1(x, Y, \phi) + \mathrm{Re}^{-1/2} v_1(x, Y, \phi) + \ldots, \\
w &= \varepsilon w_1(x, Y, \phi) + \ldots, \\
p &= -\varepsilon \ln \varepsilon + \varepsilon^2 p_1(\phi)
\end{aligned} \tag{5.2}
$$

for the velocity components and the pressure disturbances, solutions to the resulting boundary layer equations are sought in self-similar form

$$
u_1 = \frac{\partial F}{\partial \eta}(\eta, \phi), \quad w_1 = \frac{\partial \Psi}{\partial \eta}(\eta, \phi), \quad \eta = \frac{Y}{\sqrt{x}}. \tag{5.3}
$$

$F(\eta, \phi)$, $G(\eta, \phi)$ satisfy the set of equations

$$
\begin{aligned}
&-(\frac{3}{2}F + \Psi_\phi)F_{\eta\eta} + \Psi_\eta F_{\phi\eta} = F_{\eta\eta\eta}, \\
&-(\frac{3}{2}F + \Psi_\phi)\Psi_{\eta\eta} + \Psi_\eta(F_\eta + \Psi_{\phi\eta}) = -\frac{dp_1}{d\phi} + \Psi_{\eta\eta\eta}, \\
&\eta = 0 : F = \Psi = F_\eta = \Psi_\eta = 0, \\
&\eta = \infty : F_\eta = 1, \quad \Psi_\eta = 2\alpha_0 \sin\phi,
\end{aligned} \tag{5.4}
$$

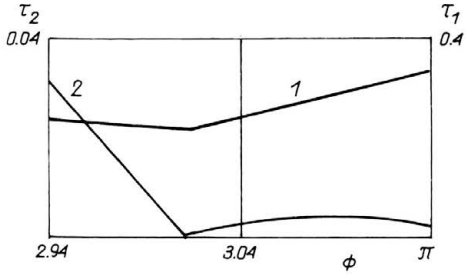

FIG. 19. Graphs τ_1, τ_2 versus Φ (ZAMETAEV [63]).

where

$$\frac{dp_1}{d\phi} = -2\alpha_0 \sin\phi(1 + 2\alpha_0 \cos\phi). \tag{5.5}$$

Equations (5.4) simplify considerably in the windward plane of symmetry $\phi = 0$ and the leeward plane of symmetry $\phi = \pi$. For example, by adopting the assumptions $w = 0$, $\partial w/\partial\phi \neq 0$ for $\phi = 0$ one obtains

$$\begin{gathered} F_{\eta\eta\eta} + \left(\frac{3}{2}F - G\right)F_{\eta\eta} = 0, \\ G_{\eta\eta\eta} + \left(\frac{3}{2}F - G\right)G_{\eta\eta} + G_\eta^2 - F_\eta G_\eta - \frac{3}{2}k\left(\frac{3}{2}k + 1\right) = 0, \\ \eta = 0 : F = G = F_\eta = G_\eta = 0, \\ \eta = \infty : F_\eta = 1, \quad G_\eta = -\frac{3}{2}k, \end{gathered} \tag{5.6}$$

where $G = \Psi/\phi$ and $k = 4\alpha_0/3$ denotes the parameter introduced by MOORE [31]. Exactly the same equation holds for $\phi = \pi$ if the definitions of G, k are modified according to $G = \Psi/(\pi - \phi)$, $k = -4\alpha_0/3$. Numerical investigations of Eqs. (5.6) have been performed by CHENG [8], ROUX [38], MURDOCK [32], CEBECI, STEWARTSON & BROWN [7] and various other authors (the reader interested in this topic is referred to RUBIN, LIN & TARULLI [39] for a useful summary). It is found that (dual) solutions exist in the windward plane $\phi = 0$ for all values of k. In contrast, similarity solutions for the leeward plane $\phi = \pi$ could be obtained for $-0.292 < k < 0$ and $-1 < k < -0.666$ only. Furthermore, integration of the full set of Eqs. (5.4), (5.5) by marching in the ϕ-direction starting with the (appropriate) windward similarity solution shows that the leeside similarity solution is recovered in the limit $\phi \to \pi$ if $0 > k > -0.292$. Moreover, these calculations indicate that the azimuthal velocity component w is no longer proportional to $(\pi - \phi)$ as $\phi \to \pi$ but rather remains finite if $-0.292 > k > -0.80$. Therefore, one of the assumptions leading to Eqs. (5.6) is violated in this range of the parameter k measuring the incidence of the cone. As a consequence, the boundary layers growing on either side of the conical tip do not blend smoothly at $\phi = \pi$ but give rise to a collision phenomenon similar to that encountered in studies dealing with high Dean number entry flows in curved ducts, STEWARTSON, CEBECI & CHANG [56], STEWARTSON & SIMPSON [57], KLUWICK & WOHLFART [23, 24]. Finally, due to the formation of a region of adverse pressure gradient $dp/d\phi > 0$ near $\phi = \pi$ for $k < -2/3$, the boundary layer separates and the numerical integration terminates before the leeside symmetry plane is reached if $k < -0.800$. The leeside similarity solutions for $k < -0.666$ thus do not appear to be of relevance, e.g. do not seem to be embedded in a global boundary-layer solution.

A detailed investigation, both numerical and analytical, of the properties of the solutions to the boundary layer equations (5.4), (5.5) has been performed by ZAMETAEV [63]. The distribution of the axial and azimuthal components of the wall shear stress $\tau_1 = F_{\eta\eta}(0, \phi)$, $\tau_2 = G_{\eta\eta}(0, \phi)$ at incipient separation $\alpha_0 = \alpha_{0c} = 0.6$ are depicted in Fig. 20. It is seen that τ_2 vanishes at $\phi = \phi_c \approx 3.01$ but the numerical integration of the boundary layer equations can be continued through this point. Furthermore the numerical results indicate that τ_2 varies linearly with ϕ as $\phi \to \phi_c$, the rates of change being different for

$\phi - \phi_c \to 0^-$ and $\phi - \phi_c \to 0^+$, however.

$$\tau_2(0, \phi) = \begin{cases} a_0(\phi_c - \phi), \phi - \phi_c \to 0^- \\ \lambda a_0(\phi - \phi_c), \phi - \phi_c \to 0^+. \end{cases} \tag{5.7}$$

Investigation of the local properties of the boundary layer equations for $|\phi - \phi_c| = O(\sigma)$, $|\alpha_0 - \alpha_{0c}| = O(\sigma^{1+\lambda})$, $\sigma \to 0$ yields

$$\tau_2(0, \phi_1) = \sigma a_0 A(\phi_1), \quad \phi_1 = \frac{\phi - \phi_c}{\sigma}, \tag{5.8}$$

where

$$(A + \phi_1)(A - \lambda\phi_1)^\lambda = G_1, \quad (A + \phi_1)(\lambda\phi_1 - A)^\lambda = G_2. \tag{5.9}$$

It is interesting to note that exactly the same result has been derived by BROWN [4] who studied the marginal separation of a three-dimensional boundary layer on a line of symmetry.

Using these relationships, which contain Eq. (5.7) as a special case $G_1 = 0$, it can be shown that $\tau_2(0, \phi)$ is a smooth function in the whole domain $-\infty < \phi_1 < \infty$ if $\alpha_0 < \alpha_{0c}$. In contrast, the wall shear stress distribution exhibits a singularity at a finite value $\phi_1 < 0$ and cannot be extended up to $\phi_1 = \infty$ if $\alpha_0 > \alpha_{0c}$. Since the strength of this singularity vanishes in the limit $\alpha_{0c} - \alpha_0 \to 0$ it can, however, be eliminated in a manner similar to the two-dimensional marginal separation case by taking into account the interaction between the boundary layer and the external inviscid flow. Comparison of the induced pressure gradient $\partial p/\partial(r\phi) = O(\sigma \mathrm{Re}^{-1/2})$ and the viscous term $\partial^2 w/\partial r^2 = O(\varepsilon\sigma^{7/4}\mathrm{Re}^{-1})$ entering the second order momentum equation following from the local analysis of the classical boundary-layer equations, indicates that the parameter range

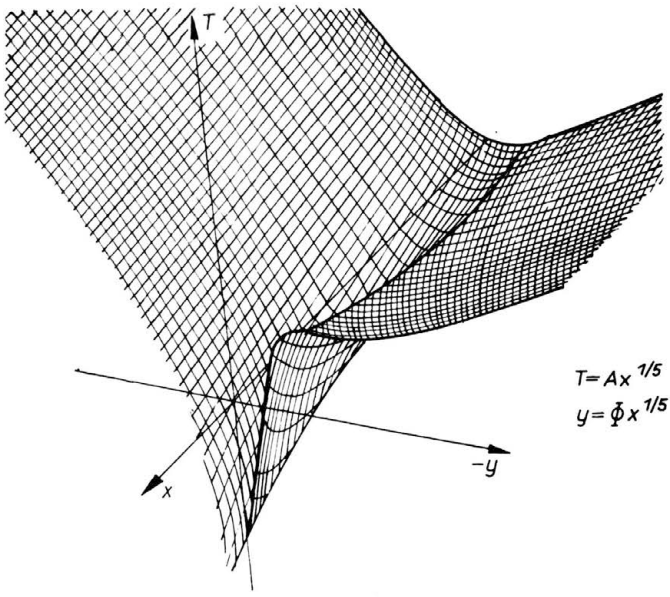

FIG. 20. Azimuthal shear stress distribution for $\Gamma = 2$, $\lambda = 0.5$ (ZAMETAEV [64]).

covered by the interaction concept is $\sigma = O(\varepsilon^{-2/5}\,\mathrm{Re}^{-1/5})$. The appropriate asymptotic interaction theory has been formulated by ZAMETAEV [64]. According to the similarity solution (5.3) the radial velocity component at the outer edge of the boundary layer is proportional to $x^{-1/2}$. As a consequence, the induced pressure disturbances inside the interaction region depend on both x and ϕ_1 which in turn forces x to occur explicitly in the expansions of the various field quantities. Viscous effects are found to be negligibly small in the main part of the boundary layer but they have to be taken into account in a thin sublayer adjacent to the wall. There the flow is governed by the three-dimensional form of the boundary-layer equations linearized with respect to the separation profile to leading order. Its solution involves an arbitrary function $B(x, \phi_1)$ characterizing the azimuthal component of the wall shear stress. In order to determine $B(x, \phi_1)$ it is necessary to derive the solvability condition for the second order equations holding in the viscous sublayer. Using suitably scaled variables A, $\overline{\phi}$ in place of B, ϕ_1 this condition can be expressed in the form, ZAMETAEV [64],

$$\int_{-\infty}^{\overline{\phi}} \left[A\frac{\partial A}{\partial t} - \lambda t + (1-\lambda)A + \frac{3}{4}(1-\lambda)x\frac{\partial A}{\partial x}\right] dt = \frac{1}{2\sqrt{x}} \int_{\overline{\phi}}^{\infty} \frac{\partial^2 A}{\partial t^2} \frac{dt}{\sqrt{t-\overline{\phi}}},$$

$$A \sim -\overline{\phi} - \Gamma(-\phi)^{-\lambda}, \quad \overline{\phi} \to -\infty, \quad A \sim \lambda\overline{\phi}, \quad \overline{\phi} \to \infty, \tag{5.10}$$

where the parameter $\Gamma \propto (\alpha_0 - \alpha_{0c})/\sigma^{1+\lambda}$ measures the incidence of the cone. As shown by ZAMETAEV [64], solutions to Eqs. (5.10) for $x \to 0$ can be expressed in terms of the similarity variable $y = x^{1/5}\overline{\phi}$: $A \sim x^{-1/5}A_1(y)$. Starting with the similarity solution Eq. (5.10) was then integrated numerically by marching in the x-direction for the two cases $\lambda = 0.5$, $\Gamma = -2$ and $\lambda = 0.5$, $\Gamma = 2$. Results for the latter case, corresponding to a value of α_0 which is larger than α_{0c}, are depicted in Fig. 20. It is seen that the minimum of the azimuthal component of the wall shear stress decreases and that the slope of the wall shear stress distribution at reattachment steepens as the distance x from the tip of the cone increases. Theoretical considerations indicate that a singularity is formed at

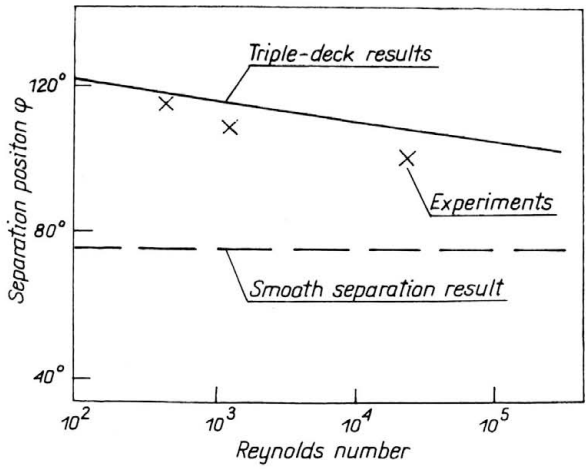

FIG. 21. Variation of the separation position Φ_S on a circular cone with Re (FIDDES [13]).

finite values of $x = x_*$, $y = y_*$ and evaluation of the numerical data yields the estimate $x_* \approx 2.3$, $y_* \approx 0.7$ for $\Gamma = 2$, $\lambda = 0.5$. It does not seem unlikely that the formation of this singularity heralds the onset of global separation characterized by the appearance of a vortex sheet shed from the point $x = x_*$, $y = y_*$. Furthermore, it may be expected that the location of the singularity moves upstream as Γ increases thus eventually leading to the case of conical separation.

The interaction process associated with the separation of a vortex sheet from a smooth conical surface has been investigated by RILEY [36], SMITH [46] generalizing earlier work by J. H. B. SMITH [45] dealing with the properties of inviscid flow. Let x, y and z denote the distance along the separation line $\phi = \phi_s$, the distance on the body surface perpendicular to this line and the distance normal to the body surface, respectively. It then follows from SMITH'S [47] work that, when y is sufficiently small, the shape of the vortex sheet leaving the surface at $y = z = 0$ can be expressed in the form $z = \mu(x)y^n$ with $n = (2M + 1)/2$. Here $M = 0, 1, \ldots$ to ensure (i) that the departure of the sheet from the body surface is tangential and (ii) that the pressure p is continuous at the sheet.

If $M = 0$ the azimuthal component of the pressure gradient exhibits a singularity as the separation line is approached from upstream $\partial p/\partial y \sim c_1(-y)^{-1/2}$, $y \to 0^-$ while $\partial p/\partial y$ vanishes in the limit $y \to 0^+$. In contrast $\partial p/\partial y$ is a smooth function of y if $M > 0$ and $\partial p/\partial y \to 0$ for $y \to 0^{\pm}$. As a consequence, the attempt to incorporate viscous effects into the inviscid flow model faces a difficulty. Owing to the strong adverse pressure gradient present for $M = 0$ the boundary layer is expected to separate upstream of the inviscid separation line $y = 0$. On the other hand it is not clear why the boundary layer separates at all if the location of the separation line is chosen such that inviscid theory predicts smooth separation $M > 0$. A similar difficulty has been encountered in studies dealing with high Reynolds number flow past circular cylinders (SYCHEV [58], SMITH [45, 47]) and as in this problem the difficulty is resolved by taking μ and c to be small rather than $O(1)$ quantities: $\mu = \mathrm{Re}^{-1/16}\bar{\mu}(x)$, $c_1 = \mathrm{Re}^{-1/16}\bar{c}_1, \bar{\mu} = O(1), \bar{c}_1 = O(1)$. Physically, this means that the separation line is shifted a small distance $\phi - \phi_s = O(\mathrm{Re}^{-1/16})$ from its inviscid position following from the requirement of smooth separation, thus introducing a weak singularity in the pressure gradient which can be smoothed out by taking into account viscous-inviscid interaction. Since $y = O(\mathrm{Re}^{-3/8})$, $z = O(\mathrm{Re}^{-3/8})$ in the local interaction region, the variation of the field quantities in the x-direction is much smaller than in the circumferential direction as well as in the direction normal to the surface, and derivations with respect to x thus drop out of the interaction equations to leading order. Similar to the case of viscous inviscid interactions on swept wing configurations (GITTLER & KLUWICK [16]), therefore, the continuity and y-momentum equations can be solved independently of the x-momentum equation which is linear in u. In terms of suitably scaled variables one then essentially recovers Eqs. (2.1), $(2.2)_1$

$$W\frac{\partial W}{\partial Y} + V\frac{\partial W}{\partial Z} = -\frac{dP}{dY} + \frac{\partial^2 W}{\partial Z^2}, \qquad \frac{\partial W}{\partial Y} + \frac{\partial V}{\partial Z} = 0,$$

(5.11)
$$W = 0 \quad \text{on} \quad Z = 0,$$
$$W \sim Z + A(Y), \quad Z \to \infty;$$
$$W \sim Z, \quad Y \to -\infty,$$

(5.12)
$$P = \frac{1}{\pi}\int_{-\infty}^{\infty} \frac{A'(\xi)}{Y - \xi}.$$

In addition to the boundary conditions (5.12), the triple-deck solution must satisfy the relationship

$$P(Y) \sim -\alpha|Y|^{1/2} \quad \text{as} \quad Y \to -\infty$$

following from the match with the pressure distribution upstream of the local interaction region. Here α denotes the scaled parameter $\bar{c}_1$ characterizing the strength of the pressure gradient singularity present there.

The success of the theoretical model outlined so far hinges on the existence of a solution to Eqs. (5.11), (5.12) and (5.13). A detailed numerical study of this nonlinear eigenvalue problem has been performed by SMITH [42]. His results strongly support the conclusion that such a solution exists and is unique, the corresponding value of α being $\alpha = 0.44$.

As pointed out earlier, the value of α determines the strength of the pressure gradient singularity occurring in the solution upstream of the triple deck region and which is smoothed out by the local interaction process. However, it also determines the local shape of the vortex sheet leaving the body surface as well as the position of the separation line, Fig. 21.

Equations (5.11), (5.12) and (5.13) provide a self-consistent description of the local flow properties near the separation line of a conical vortex sheet. Unfortunately, however, attempts to embed this local structure into the global flow field are faced with severe difficulties. These difficulties are associated with the behaviour of the boundary layer downstream of the triple-deck region which, due to the curvature of the external streamlines, develops a jet-like velocity profile. SMITH [46] argues that the boundary layer, therefore, must separate before it reaches the triple-deck region to shelter the decelerating fluid in the lower deck from the faster upstream moving fluid. This in turn leads to the formation of another separated sheet and it is not yet clear how the merging between this sheet and that emanating from the triple deck can be achieved.

6. Concluding remarks

It has been shown that asymptotic methods provide a useful tool for the investigation of interacting laminar boundary layers on axisymmetric bodies. Applications include the flow past cylindrical bodies with slightly perturbed surfaces, trailing tip flows and the flow past cones at incidence. These contributions have considerably deepened the current knowledge of the properties of high Reynolds number laminar flows. However, in a number of cases only the first steps towards a consistent asymptotic theory have been made and important problems remain unsolved. For example, it is not clear yet how the transition from local to global separation takes place both in cases without and with incidence. Although the behaviour of the classical boundary layer near the trailing tip of an axisymmetric body has been elucidated quite recently assuming that the body shape is given by a power law, the interaction equations have been formulated and solved only for a very narrow regime of the exponent so far. Interesting progress has been achieved as far as the flow past a slender cone at incidence is concerned. Clearly, however, a more detailed numerical study of the resulting equation for marginal (cross-flow) separation concentrating on the possibility of multiple solutions also seems desirable. Furthermore, a complete picture of the flow will have to include a more

refined model of the collision phenomenon which sets in before crossflow separation occurs.

This research was supported in part by the Austrian FWF under grant number P5557 and jointly by FWF and the National Science Foundation under grant number P5825.

References

1. H. Bippes and M. Turek, *Oil flow patterns of separated flow on a hemisphere-cylinder at incidence*, DFVLR FB 84–20, 1984.
2. R. J. Bodonyi and A. Kluwick, *Viscous inviscid interaction on a slender axisymmetric trailing tip flow*, in preparation.
3. R. J. Bodonyi, F. T. Smith and A. Kluwick, *Axisymmetric flow past a slender body of finite length*, Proc. Roy. Soc. London, **A 400**, pp. 37–54, 1985.
4. S. N. Brown, *Marginal separation of a three-dimensional boundary layer on a line of symmetry*, J. Fluid Mech., **158**, pp. 95–111, 1985.
5. S. N. Brown and K. Stewartson, *On an integral equation of marginal separation*, SIAM J. Appl. Math., **43**, 5, pp. 1119–1126, 1983.
6. W. B. Bush, *Axial incompressible flow past a body of revolution*, Rocky Mt. J. Math., **6**, pp. 527, 1976.
7. T. C. Cebeci, K. Stewartson and S. N. Brown, *Nonsimilar boundary layers on the leeside of cones at incidence*, Comp. Fluids, **11**, pp. 175–186, 1983.
8. H. K. Cheng, *The shock layer concept and three-dimensional hypersonic boundary layers*, Cornell. Aero. Lab. Rept., AF–1285–A–3, 1961.
9. J. D. Cole, *Perturbation methods in applied mathematics*, Blaisdell Publ. Comp., 1968.
10. U. Dallmann, *Topological structures of three-dimensional separations*, DFVLR FB,221–82–A07, 1982.
11. P. W. Duck, *The effect of a surface discontinuity on an axisymmetric boundary layer*, Q. J. Mech. Appl. Math., **37**, pp. 57, 1984.
12. P. W. Duck and O. Burggraf, *Spectral solutions for three-dimensional triple-deck flow over surface topography*, J. Fluid Mech., **162**, pp. 1–22, 1986.
13. S. P. Fiddes, *A theory of separated flow past a slender elliptic cone at incidence*, AGARD C-P paper 30, Sept/Oct., Colorado Springs, 1980.
14. M. B. Glauert and M. J. Lighthill, *The axisymmetric boundary layer on a long thin cylinder*, Proc. Roy. Soc. London, **A 230**, pp. 113, 1955.
15. Ph. Gittler and A. Kluwick, *Triple-deck solutions for supersonic flows past flared cylinders*, J. Fluid Mech., **179**, pp. 469– 487, 1987.
16. Ph. Gittler and A. Kluwick, *Interacting laminar boundary layers in quasi-two-dimensional flow*, Fluid Dyn. Res., **5**, pp. 29–47, 1989.
17. H. G. Hornung and A. E. Perry, *Some aspects of three-dimensional separation. Part I. Streamsurface bifurcation*, Z. Flugwiss. Weltraumforsch., **8**, pp. 77–78, 1984.
18. H. P. Horton, *Adiabatic laminar boundary-layer/shock-wave interactions on flared axisymmetric bodies*, AIAA J., **9**, pp. 2141–2148, 1971.
19. A. Kluwick, *Interacting boundary layers*, Z. Angew. Math. Mech., **67**, T3–13, 1987.
20. A. Kluwick, *Marginal separation of laminar axisymmetric boundary layers*, Z. Flugwiss. Weltraumforsch., **13**, pp. 254–259 [in German], 1989.
21. A. Kluwick, Ph. Gittler and R. J. Bodonyi, *Viscous-inviscid interactions on axisymmetric bodies of revolution in supersonic flow*, J. Fluid Mech., **140**, pp. 281–301, 1984.
22. A. Kluwick, Ph. Gittler and R. J. Bodonyi, *Freely interacting axisymmetric boundary layers on bodies of revolution*, Q. J. Mech. Appl. Maths, **38**, pp. 575–588, 1985.
23. A. Kluwick and H. Wohlfart, *Entry flow in weakly curved ducts*, Ingenieur-Archiv, **54**, pp. 107–120, 1984.
24. A. Kluwick and H. Wohlfart, *Hot-wire-anemometer study of the entry flow in a curved duct*, J. Fluid Mech., **165**, pp. 335–353, 1986.
25. R. Leblanc and J. Ginoux, *Influence of cross flow on two-dimensional separation*, Von Kármán Institute for Fluid Dynamics, TN 62, 1970.
26. R. Legendre, *Séparation de l'ecoulement laminaire tridimensionnel*, La Rech. Aéronaut., **54**, pp. 3–8, 1956.

27. M. J. LIGHTHILL, *Attachment and separation in three-dimensional flow*, In: L. ROSENHEAD [Ed.], Laminar Boundary Layers, pp. 72–82, Oxford Univ. Press, Oxford 1963.
28. F. T. SMITH and J. H. MERKIN, *Triple deck solutions for subsonic flow past humps, steps, concave or convex corners and wedged trailing edges*, Comp. Fluids, **10**, pp. 7–25, 1982.
29. A. F. MESSITER, *Boundary layer flow near the trailing edge of a flat plate*, SIAM J. Appl. Math., **18**, pp. 241–257, 1970.
30. A. F. MESSITER, *Boundary-layer interaction theory*, ASME J. Appl. Mech., **50**, 1983.
31. F. K. MOORE, *Laminar boundary layer on cone in supersonic flow at large angle of attack*, NACA Rept., 1132, 1953.
32. J. W. MURDOCK, *The solution of sharp-cone boundary-layer equations in the plane of symmetry*, J. Fluid Mech., **54**, pp. 665–678, 1972.
33. V. Ya. NEILAND, *Asymptotic theory of the separation and the boundary layer supersonic gas flow interaction*, Adv. in Mech. **4**, pp. 1–62, 1981.
34. K. OSWATITSCH, *Die Ablösebedinungen von Grenzschichten*, In: Grenzsschichtforschung, [Ed.] H. GÖRTLER, IUTAM Symp., Freiburg 1957, pp. 357–367, Springer 1958.
35. A. E. PERRY and M. S. CHONG, *A series-expansion study of the Navier-Stokes equations with applications to three-dimensional separation patterns*, J. Fluid Mech., **173**, pp.207–223, 1986.
36. N. RILEY, *Separation from a smooth surface in a slender conical flow*, J. Eng. Math., **13**, pp. 75–91, 1979.
37. D. P. RIZZETTA, O. R. BURGGRAF and R. JENSON, *Triple-deck solutions for viscous supersonic and hypersonic flow past corners*, J. Fluid Mech., **89**, pp. 535–552, 1978.
38. B. ROUX, *Supersonic laminar boundary layer near the plane of symmetry of a cone at incidence*, J. Fluid Mech., **51**, pp. 1–14, 1972.
39. S. G. RUBIN, T. C. LIN and F. TARULLI, *Symmetry plane viscous layer on a sharp cone*, AIAA J., **15**, pp. 204–211, 1977.
40. A. I. RUBAN, *Singular solutions of boundary layer equations which can be extended continuously through the point of zero surface friction*, Izv. Akad. Nauk SSSR, Mekh. Zhidk. Gaza, **6**, pp. 42–52, 1981.
41. A. I. RUBAN, *Asymptotic theory of short separation regions on the leading edge of a slender airfoil*, Izv. Akad. Nauk SSSR, Mekh. Zhidk. Gaza, **1**, pp. 42–51, 1981.
42. J. H. B. SMITH, *Behaviour of a vortex sheet separating from a smooth surface*, RAE TR 77058, pp. 62, 1977.
43. F. T. SMITH and P. DUCK, *Separation of jets or thermal boundary layers from a wall*, Q. J. Mech. Appl. Math., **30**, pp. 143, 1977.
44. F. T. SMITH, R. I. SYKES and P. W. M. BRIGHTON, *A two- dimensional boundary layer encountering a three-dimensional hump*, J. Fluid Mech., **83**, pp. 163–176, 1977.
45. F. T. SMITH, *The laminar separation of an incompressible fluid streaming past a smooth surface*, Proc. Roy. Soc. London, **A 356**, pp. 433–463, 1977.
46. F. T. SMITH, *Three-dimensional viscous and inviscid separation of a vortex sheet from a smooth non-slender body*, RAE TR 78095, pp. 33, 1978.
47. F. T. SMITH, *Laminar flow of an incompressible fluid past a bluff body: the separation, reattachment, eddy properties and drag*, J. Fluid Mech., **92**, pp. 171–205, 1979.
48. F. T. SMITH, *On the high Reynolds number theory of laminar flows*, IMA J. Appl. Maths., **28**, pp. 207–281, 1982.
49. F. T. SMITH, *A reversed flow singularity in interacting boundary layers*, Proc. Roy. Soc. London, **A 420**, pp. 21–52, 1988.
50. K. STEWARTSON, *The asymptotic boundary layer on a circular cylinder in axial incompressible flow*, Q. Appl. Math., **13**, p. 113, 1955.
51. K. STEWARTSON, *On the flow near the trailing edge of a flat plate II*, Mathematika, **16**, pp. 106–121, 1969.
52. K. STEWARTSON, *On laminar boundary layers near corners*, Q. J. Mech, Appl. Math., **23**, pp. 137–152, 1970.
53. K. STEWARTSON, *Corrections and an addition*, Q. J. Mech. Appl. Math., **24**, pp. 387–389, 1971.
54. K. STEWARTSON, *Multistructured boundary layers on flat plates and related bodies*, Adv. Appl. Mech., **14**, pp. 145–239, 1974.
55. K. STEWARTSON, F. T. SMITH and K. KAUPS, *Marginal separation*, Stud. Appl. Math., **67**, pp. 45–61, 1982.
56. K. STEWARTSON, T. C. CEBECI and K. C. CHANG, *A boundary-layer collision in a curved duct*, Q. J. Mech. Appl. Math., **33**, pp. 59–75, 1980.
57. K. STEWARTSON and C. J. SIMPSON, *On a singularity initiating a boundary-layer collision*, Q. J. Mech. Appl. Math., **35**, pp. 1–16, 1982.
58. V. V. SYCHEV, *On laminar separation*, Izv. Akad. Nauk SSSR, Mekh. Zhidk. Gaza, **3**, p. 47, 1972.

59. R. I. SYKES, *On the three-dimensional boundary layer flow over surface irregularities*, Proc. Roy. Soc. London, A **373**, pp. 311–329, 1980.
60. S. M. TIOMSHIN, Utscheni Zapisski Zag., **16**, pp. 10–21, 1985.
61. S. M. TIOMSHIN, Utscheni Zapisski Zag., **17**, pp. 33–41, 1986.
62. V. VATSA and M. WERLE, *Quasi-three-dimensional laminar boundary layer separations in supersonic flow*, Trans. ASME, J. Fluid Engng., **99**, pp. 634–639, 1977.
63. V. B. ZAMETAEV, *Singular solution of equations of a boundary layer on a slender cone*, Izv. Akad. Nauk SSSR, Mekh. Zhidk. Gaza, **2**, pp. 65–72, 1986.
64. V. B. ZAMETAEV, *Local separation on a slender cone preceding the appearance of a vortex sheet*, Izv. Akad. Nauk SSSR, Mekh. Zhidk. Gaza, **6**, pp. 21–28, 1987.

INSTITUT FÜR STRÖMUNGSLEHRE UND WÄRMEÜBERTRAGUNG
TECHNISCHE UNIVERSITÄT, WIEN. ÖSTERREICH.

Received August 26, 1991.